Tropospheric Water Vapor Profiles Retrieved from Pressure-Broadened Emission Spectra at 22 GHz

ALEXANDER HAEFELE

Institute of Applied Physics, University of Bern, Bern, Switzerland

NIKLAUS KÄMPFER

Institute of Applied Physics, and Oeschger Center for Climate Change Research, University of Bern, Bern, Switzerland

(Manuscript received 20 May 2009, in final form 4 August 2009)

ABSTRACT

The authors present the analysis and the evaluation of the retrieval of tropospheric water vapor profiles from pressure-broadened emission spectra at 22 GHz measured with a ground-based microwave spectroradiometer. The spectra have a bandwidth of 1 GHz with a resolution of 20 MHz and are centered at 22.235 GHz. Because of the small bandwidth, the retrieval is insensitive to clouds and measurements are possible under almost all nonprecipitating weather conditions. The retrieved profiles are evaluated with a set of 200 coincident balloon soundings with RS92 sensors. The correlation coefficient between the microwave retrievals and the RS92 measurements lies above 0.7 km, up to 8 km, and the retrievals show a wet bias compared to RS92 of 10% at 2 km, increasing to 30% at 6 km.

1. Introduction

Water vapor is the most important natural greenhouse gas of the atmosphere and has a large impact on its radiative properties and hence on its thermodynamic balance. Despite the importance of water vapor in the climate system and weather forecasting, there is no technique available, neither ground-based nor spaceborne, that can provide continuous measurements of the humidity profile under all weather conditions. Ground-based microwave radiometers measuring the pressure-broadened emission line of water vapor at 22 GHz are good candidates to fill this gap.

Classical microwave profilers usually cover a frequency range from 20 to 30 GHz at a few individual channels for humidity measurements (Solheim et al. 1998; Crewell et al. 2001; Ware et al. 2003; Martin et al. 2006). The instrument presented here, however, was originally designed to measure water vapor profiles in the stratosphere and mesosphere as part of the Network for the Detection of Atmospheric Composition Change (NDACC; available online at http://www.ndacc.org). It covers a bandwidth of 1 GHz centered at 22.235 GHz with very high spectral resolution of 61 kHz, as required for observations in the middle atmosphere. Thus, only the peak of the H_2O line is measured, as shown in Fig. 1. The spectral signature of clouds within the measured frequency interval of 1 GHz is in good approximation linear in frequency. The forward calculation in the retrieval is therefore based on a clear-sky atmosphere, and clouds are accounted for by adding an offset and a slope to the calculated spectrum. This approach allows the retrieval of water vapor profiles under almost all nonprecipitating weather conditions without additional information on clouds.

The paper is organized as follows: A short description of the instrument and the calibration method is presented in section 2. In section 3, the retrieval is discussed and the key characteristics are derived. A validation of the retrievals is presented in section 4.

2. Instrument and calibration

The emission spectra are measured by the Middle Atmospheric Water Vapor Radiometer (MIAWARA;

Corresponding author address: Alexander Haefele, Institute of Applied Physics, University of Bern, Sidlerstrasse 5, 3014 Bern, Switzerland.
E-mail: haefele@iap.unibe.ch

DOI: 10.1175/2009JTECHA1334.1

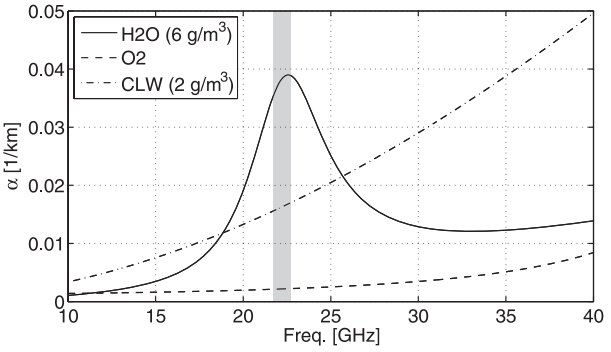

FIG. 1. Absorption coefficient between 10 and 40 GHz at 850 hPa for water vapor, cloud liquid water, and oxygen. The shaded area marks the bandwidth of the radiometer.

Deuber et al. 2004), which is optimized for measuring the narrowband emission line from stratospheric and mesospheric water vapor. MIAWARA was developed and is operated by the University of Bern and is deployed close to Bern, Switzerland, at 47°N, 7°E at 900 m MSL. It is a single sideband heterodyne receiver converting the incoming signal at 22.235 GHz to an intermediate frequency of 0.5 GHz in two mixing steps. The signal is analyzed by a digital fast Fourier transform spectrometer with a spectral range from 0 to 1 GHz and a resolution of 61 kHz. Hence, the radiometer system is able to measure the emission from water vapor at frequencies between 21.735 and 22.735 GHz at very high resolution, as required for observations in the middle atmosphere. This high resolution, however, is of no advantage for the retrieval of tropospheric profiles, and for this study the high resolution raw spectra are binned into 20-MHz bins before being calibrated.

The instrument is calibrated with a tipping curve measurement (Han and Westwater 2000) that is performed every half an hour. The tipping curve includes six antenna positions per measurement cycle looking at 1) a microwave absorber at ambient temperature (referred to as hot load) and at the sky under zenith angles ϕ = [30°; 36°; 42°; 48°; 54°]. Assuming an isothermal and stratified atmosphere, the brightness temperature under a zenith angle ϕ is given by

$$\mathrm{Tb}_{\mathrm{sky}}(\phi) = T_{\mathrm{bg}} e^{-\tau/\cos(\phi)} + T_{\mathrm{eff}}[1 - e^{-\tau/\cos(\phi)}], \qquad (1)$$

where T_{bg} is the cosmic background radiation; T_{eff} is the effective temperature of the atmosphere, derived from the ambient surface temperature T_{amb}; $T_{\mathrm{eff}} = 0.69(T_{\mathrm{amb}} - 273) + 266.3$ according to Han and Westwater (2000); and τ is the atmospheric opacity in zenith direction. On the other hand, we can write the total power calibration assuming to know the brightness temperature of the sky at a reference angle ϕ_{ref}:

$$\mathrm{Tb}_{\mathrm{sky}}(\phi) = [S_{\mathrm{sky}}(\phi) - S_{\mathrm{sky}}(\phi_{\mathrm{ref}})] \frac{T_{\mathrm{hot}} - \mathrm{Tb}_{\mathrm{sky}}(\phi_{\mathrm{ref}})}{S_{\mathrm{hot}} - S_{\mathrm{sky}}(\phi_{\mathrm{ref}})} + \mathrm{Tb}_{\mathrm{sky}}(\phi_{\mathrm{ref}}), \qquad (2)$$

where $S_{\mathrm{sky}}(\phi)$ is the signal from the sky measured at a zenith angle ϕ and S_{hot} is the signal from the hot load. Iterating Eqs. (1) and (2) until they are fulfilled for all zenith angles of the tipping curve yields τ. From numerical simulations, the systematic error of τ is estimated to be 5%. Equation (1) is used to calculate $\mathrm{Tb}(\phi_{\mathrm{ref}})$, *and the error in* τ *converts to an error in* $\mathrm{Tb}(\phi_{\mathrm{ref}})$ *of 3 K. The random error depends strongly on* the atmospheric conditions, because the atmosphere is assumed to be homogeneously layered. If strong horizontal gradients in the distribution of water vapor are present, the random error is on the order of a few kelvins while it is below 1 K for a well-stratified atmosphere. The receiver temperature can also be derived from tipping curve measurements and lies at 140 ± 5 K. This is in agreement with the value derived from calibrations with a liquid nitrogen load. Tipping curves that reveal a receiver temperature of $T_{\mathrm{rec}} < 120$ K or $T_{\mathrm{rec}} > 160$ K are rejected.

The thermal noise on a binned, single spectrum derived from a tipping curve is 0.2 K. For this study, bunches of 16 spectra have been summed up before the retrieval is performed to reduce the noise to 0.05 K. Because tipping curves are performed only every half an hour, the retrieved profiles are averaged over 8 h.

3. Retrieval of water vapor profiles

An optimal estimation algorithm according to Rodgers (2000) is applied to retrieve water vapor profiles from the pressure-broadened emission spectra. Given a state vector **x** and an additional set of parameters **b**, the measured radiation spectrum **y** is calculated with the forward model *F*:

$$\mathbf{y} = F(\mathbf{x}, \mathbf{b}). \qquad (3)$$

The state vector **x** is the quantity to be retrieved and contains the water vapor profile, and **b** contains parameters describing the sensor; spectroscopic parameters; pressure and temperature profiles; and profiles of O_2, N_2, and CO_2. For the radiative transfer calculations and for the sensor modeling the software packages Atmospheric Radiative Transfer Simulator (ARTS; Buehler et al. 2005) and QPack (Eriksson et al. 2005) have been used. In fact, within ARTS the absorption coefficients are calculated with the model PWR98 (Rosenkranz 1998). Pressure and temperature profiles are taken from

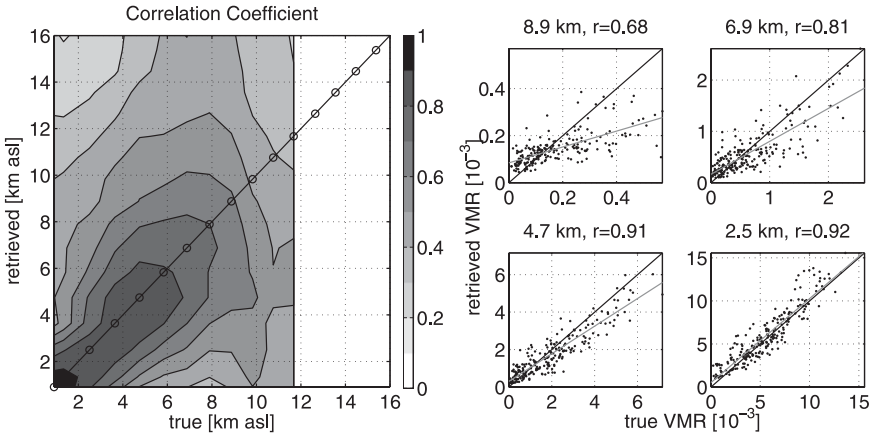

FIG. 2. Analysis of the simulated retrievals. (left) Matrix of correlation coefficients between the true and the retrieved profiles. Because the true profiles are based on RS92 measurements, they are only taken into account up to 11.5 km. (right) Scatterplots of the true and the retrieved data, where r is the correlation coefficient.

European Centre for Medium-Range Weather Forecasts (ECMWF) reanalyses. Estimating the state vector $\hat{\mathbf{x}}$, given the measured radiation spectrum $\mathbf{y}$, is the inverse problem. Because there exists an infinite number of states that solve the inverse problem, the solution has to be constrained to realistic profiles. From the Bayes theorem, the following cost function can be derived:

$$c = [\mathbf{y} - F(\hat{\mathbf{x}})]^{\mathrm{T}} \mathbf{S}_{\mathbf{y}}^{-1} [\mathbf{y} - F(\hat{\mathbf{x}})] + [\hat{\mathbf{x}} - \mathbf{x}_{\mathbf{a}}]^{\mathrm{T}} \mathbf{S}_{\mathbf{a}}^{-1} [\hat{\mathbf{x}} - \mathbf{x}_{\mathbf{a}}], \tag{4}$$

where $\mathbf{x_a}$ is an a priori assumption of the water vapor profile, the a priori profile, and $\mathbf{S_a}$ is the error covariance of $\mathbf{x_a}$ controlling the strength of the constraint of the solution $\hat{\mathbf{x}}$ to the a priori profile. The solution of the inverse problem $\hat{\mathbf{x}}$ minimizes the cost function c. Because F is nonlinear in the troposphere with respect to $\mathbf{x}$, an iterative search for the solution $\hat{\mathbf{x}}$ is required and a Marquardt–Levenberg approach is used.

Within the spectral range of 1 GHz, the contribution from clouds to the measured brightness temperature can be reasonably well approximated with a linear term in the forward model. Thus, a polynomial of degree one is included in the forward model to account for clouds, and its coefficients (offset and slope) are part of the state vector $\mathbf{x}$.

Our a priori assumptions are as follows: The a priori profile $\mathbf{x_a}$ decreases linearly from the surface volume mixing ratio, obtained from relative humidity and temperature measurements of the nearby weather station, to the statistical mean value at 500 hPa. Above this altitude, the a priori profile is equal to the statistical mean profile, which has been derived from one year of balloon soundings close to the measurement site. The a priori covariance matrix $\mathbf{S}_a$ is calculated from the standard deviations $\sigma(i)$ and the correlation lengths $l_c(i)$ at the altitudes $z(i)$ assuming Gaussian statistics:

$$\mathbf{S}_a(i,\ j) = \sigma(i)\sigma(j) \exp\left\{-4\left[\frac{z(i) - z(j)}{l_c(i) + l_c(j)}\right]^2\right\}. \tag{5}$$

The a priori standard deviation is expressed as fraction of the a priori profile and is set to 10% at the surface increasing to 80% at 500 hPa and staying constant at 80% above. The correlation length is set to 2 km (one scale height of water vapor). The a priori values of the offset and slope are set to zero, whereas the standard deviations are set to 9 K and 0.2 K Hz^{-1}, respectively.

For the characterization of the retrieval, a simulation has been performed. From a set of 241 balloon soundings, we calculated synthetic spectra that were subsequently inverted using the approach and a priori information as described earlier. Gaussian noise with a standard deviation of 0.01 K was added to the spectra before inversion. It has to be noted that this low noise is not achieved by the real measurement within reasonable integration times, because tipping curves are performed only every half hour. The simulation should be regarded as representative for the best performance that could be achieved by this approach. Liquid water clouds have been included in the radiative transfer for the calculation of the synthetic spectra. The profile of the liquid water content ρ was built according to the following rule:

$$\rho = \begin{cases} 0.2\,\mathrm{g\,m^{-3}} & \text{for} \quad \mathrm{RH} > 95\% \\ 0\,\mathrm{g\,m^{-3}} & \text{for} \quad \mathrm{RH} \le 95\% \end{cases}. \tag{6}$$

TABLE 1. Random error (std dev of differences between retrieved and true profiles) of the water vapor retrievals derived from the simulation (VMR is the volume mixing ratio).

Height (km MSL)	Relative (%)	Absolute (VMR)	Absolute ($g\ m^{-3}$)
1	5	7×10^{-4}	0.5
4	30	1×10^{-3}	0.5
6	45	5×10^{-4}	0.2
9	55	1×10^{-4}	0.03

In the retrieval, however, the clouds were accounted for with a first-order polynomial as described earlier. The comparison of the true profile with the retrieved profile gives insight in the characteristics of the retrieval. The left panel of Fig. 2 shows the correlation coefficient between the true and the retrieved profiles. The high correlation in the first kilometer comes mainly from the influence of the a priori profile that is set to the measured surface value at the ground, as described earlier. Experiments with a constant a priori profile reveal significantly lower correlation between 1 and 2 km (not shown). The correlation length, here defined as the distance over which the correlation coefficient decreases below 0.5, gives an indication of the vertical resolution. Up to an altitude of 6 km, the correlation length is ≈5 km. For this analysis, the data have been deseasonalized by subtracting a second-order polynomial fit from the one-year data record. The seasonal cycle would introduce substantial correlations throughout the whole troposphere. It has to be noted also that the correlation length of water vapor measured by radiosondes is 2 km. The right panels in Fig. 2 show the scatterplots of the retrieved and the true atmosphere at four pressure levels. The retrieval performs well up to 7 km. At 9 km, high values are underestimated, which is due to the increasing influence of the a priori profile. Including a seasonal cycle in the a priori profile improves the performance of the levels at 8 and 9 km noticeably (not shown).

The random error (standard deviation of the differences between retrieved and true profile; see Fig. 2, right) is 5% of the mean value at the surface and increases linearly to 55% at 9 km. This corresponds to precisions given in Table 1, which compare well with the numbers reported by Crewell et al. (2001) for a 22-channel radiometer (10 water vapor channels).

We note that the retrieved offset and slope, which are expected to account for the effect of clouds, correlate well with the integrated liquid water. The correlation coefficients are $r = 0.65$ and $r = 0.61$ for the offset and the slope, respectively.

4. Results

Within 15 km distance to the site, where the radiometer is operated, 3–4 balloon soundings per week were performed during the time period from June 2007 to June 2008. The balloon payload was equipped with a Vaisala RS92 sensor. This dataset is used to evaluate the water vapor retrievals from the ground-based radiometer. An assessment of the accuracy of RS92 is presented by Miloshevich et al. (2009), and good agreement of nighttime measurements with the Cryogenic Frostpoint Hygrometer (CFH; Vömel et al. 2007), within 10% up to 5 km, is reported. However, a strong dry bias of daytime RS92 soundings compared to CFH of up to 30% at 10 km is reported. We corrected for this bias by applying the radiation correction suggested by Miloshevich et al. (2009)

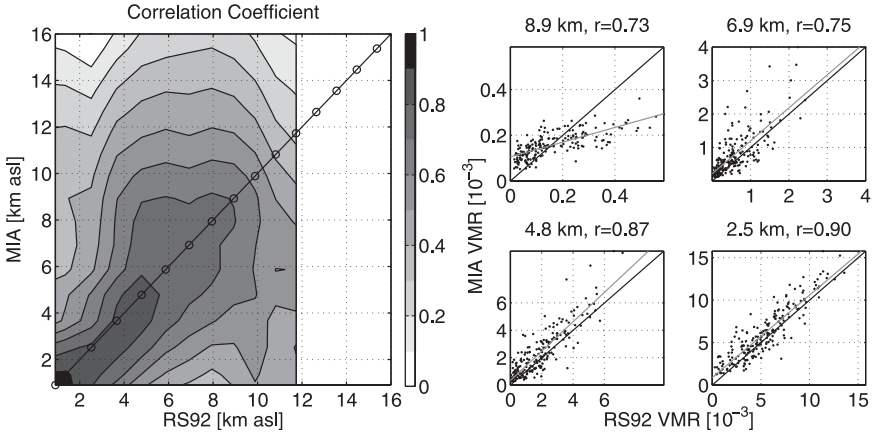

FIG. 3. Analysis of the real retrievals. (left) Matrix of correlation coefficients between RS92 and the microwave retrievals (MIAWARA). RS92 measurements are only taken into account up to 11.5 km. (right) Scatterplots of RS92 and radiometer data, where r is the correlation coefficient. RS92 profiles have been corrected for the radiation dry bias (see section 4).

to the RS92 measurements, because all soundings considered in this study were performed during day. The correction is a function of pressure and solar zenith angle. Because clouds are expected to significantly reduce the radiation error, the correction was only applied to those portions of the RS92 humidity profiles that were lying above the uppermost cloud layers. Clouds are assumed in regions where the relative humidity is >95%.

The left panel of Fig. 3 shows the correlation coefficients between the retrievals, based on the measured spectra, and the coincident balloon soundings. Again, the seasonal cycle has been subtracted from the data for this analysis. The correlation matrix is in good agreement with the one derived from the simulation (Fig. 2). The scatterplots of the retrievals and RS92 measurements are shown in the right panels of Fig. 3. The performance of the retrieval is good up to 5 km, with the restriction that high values are slightly overestimated. At 6 and 7 km, the correlation is degraded and a wet bias is noted. At 8 and 9 km, the retrieval is not able to get the high values right at this altitude because of the increasing influence of the a priori profile. As mentioned in section 3, including a seasonal cycle in the a priori profile would improve the performance at these levels.

Figure 4 shows time series of water vapor measured by RS92 and by the radiometer at four pressure levels. The features discussed earlier are evident, namely the high correlation between the two datasets and the wet bias of the microwave retrievals compared to RS92. Visual inspection of the time series reveals that the agreement is generally better after September 2007 (most pronounced at 420 hPa). In September 2007, the radiometer experienced a few hardware changes, including the installation of a blade to protect the hot load (ambient load) from direct insolation. This leads to a better definition of the temperature of the hot load, and thus improves the calibration. We are not able to quantify the effect of these changes on the retrievals, but we note that they improved the calibration and are likely to explain the better performance after September 2007.

In the following analysis, we consider only data after September 2007, which reduces the total of 208 profile pairs to a total of 145. The mean of the differences between the radiometer and RS92 as a function of altitude is presented in the left panel of Fig. 5. A wet bias of 10%–20% is apparent at altitudes below 6 km. The random error (standard deviation of the differences between radiometer and RS92) is shown in the right panel of Fig. 5, along with the natural variability (dashed line) and the random error of the a priori profile (dashed–dotted line). Because the a priori profile is set to the measured surface value at the ground, it performs slightly better than the retrieval up to 2 km. Above 2 km, information

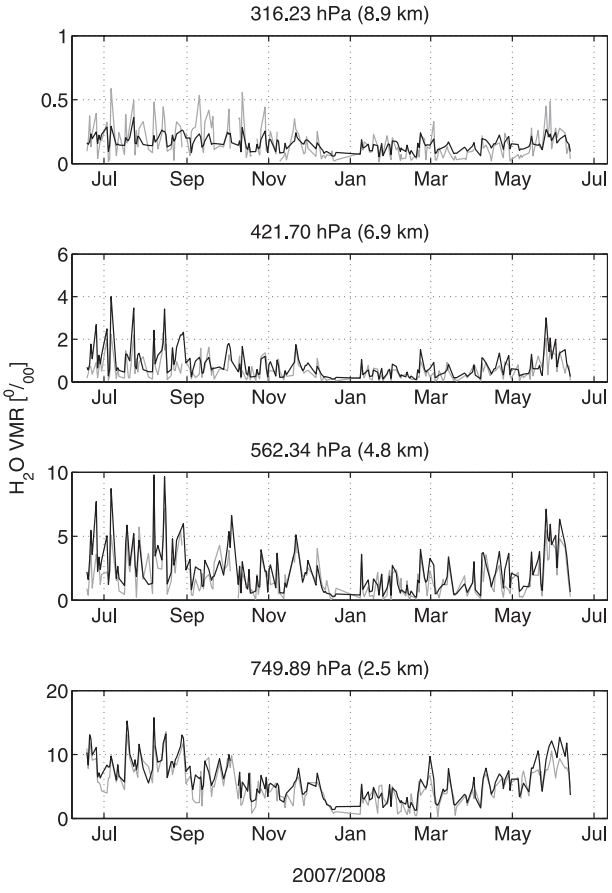

FIG. 4. Time series of H_2O mixing ratio as measured by RS92 (gray lines) and the ground-based microwave radiometer (black lines) at four different pressure levels. RS92 profiles have been corrected for the radiation dry bias (see section 4).

from the measurement is added to the a priori profile and the retrieval performs well up to 9 km, showing a bump in the random error profile reflecting decreased correlation with RS92 at 6–7 km. The random error of the retrievals is in good agreement with the one derived from the simulation.

The temperature profiles from ECMWF are on average 1.5 K warmer than the temperatures measured by the radiosonde. Using the temperature profiles from the radiosonde in the retrieval increases, the bias in water vapor of the microwave retrievals compared to RS92 by 1%–2%.

5. Summary and conclusions

We presented a characterization and first results of the retrieval of tropospheric water vapor profiles from pressure-broadened emission spectra. The measured spectra have a bandwidth of 1 GHz at a resolution of 20 MHz and are centered at 22.235 GHz. This is in

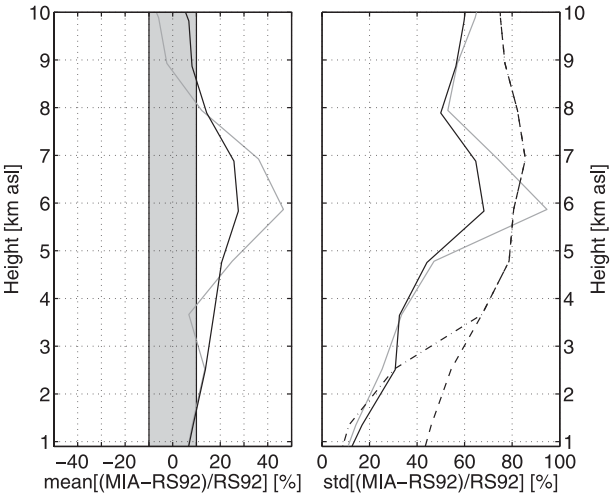

FIG. 5. (left) Mean and (right) std dev of the relative differences between the radiometer (MIAWARA) and RS92 profiles considering only measurements after 1 Oct 2007 (solid black line; 145 profiles) and considering all measurements (solid gray line; 203 profiles). (right) The natural variability of water vapor (dashed line) and the random error of the a priori (dashed–dotted line) are also displayed.

contrast to conventional microwave profilers, which cover a broader spectral range at a much coarser resolution. The spectra are calibrated by means of a tipping curve measurement and inverted with an optimal estimation algorithm, because the small-bandwidth clouds can be accounted for with an offset and a slope in the forward model and no additional information on clouds is needed. This is a major advantage of this approach, because water vapor profiles of good quality can be retrieved under almost all nonprecipitating weather conditions.

A simulation of the retrieval demonstrates the potential of this experimental setup and shows that measurements are in principle possible up to 9 km with a vertical resolution of ≈5 km. This performance is comparable to conventional microwave profilers. The real measurements have been evaluated with 200 coincident balloon soundings. The RS92 data have been corrected for the radiation dry bias. The performance of the real retrieval is good throughout the whole troposphere, showing a correlation with RS92 better than 0.7. Best performance is found up to the middle troposphere (5 km). The random error derived from the measurements is 10% at the surface and increases to 55% at 9 km. In general, the retrieved profiles show a wet bias compared to RS92 of 10%–20% between 2 and 5 km. This wet bias is substantial and needs to be investigated further. We note that, in the retrieval, water vapor is assumed to be normally distributed. This assumption is questionable and could introduce a bias. However, we conclude that this unconventional setup is well suited to measure tropospheric humidity up to 9 km, independent from additional cloud information under a large range of weather conditions.

Acknowledgments. This work has been supported by the Swiss National Science foundation under Grant 200020-115882/1 as well as through the project SHOMING financed by MeteoSwiss within GAW. We acknowledge the support of the European Commission through the GEOMON Integrated Project under the 6th Framework Program (Contract FOP6-2005-Global-4-036677).

REFERENCES

Buehler, S. A., P. Eriksson, T. Kuhn, A. von Engeln, and C. Verdes, 2005: ARTS, the atmospheric radiative transfer simulator. *J. Quant. Spectrosc. Radiat. Transf.,* **91,** 65–93, doi:10.1016/j.jqsrt.2004.05.051.

Crewell, S., H. Czekala, U. Löhnert, C. Simmer, T. Rose, R. Zimmermann, and R. Zimmermann, 2001: Microwave Radiometer for Cloud Carthography: A 22-channel ground-based microwave radiometer for atmospheric research. *Radio Sci.,* **36,** 621–638.

Deuber, B., N. Kämpfer, and D. Feist, 2004: A new 22-GHz radiometer for middle atmospheric water vapour profile measurements. *IEEE Trans. Geosci. Remote Sens.,* **42,** 974–984.

Eriksson, P., C. Jiménez, and S. A. Buehler, 2005: Qpack, a general tool for instrument simulation and retrieval work. *J. Quant. Spectrosc. Radiat. Transf.,* **91,** 47–64, doi:10.1016/j.jqsrt.2004.05.050.

Han, Y., and E. R. Westwater, 2000: Analysis and improvement of tipping calibration for ground-based microwave radiometers. *IEEE Trans. Geosci. Remote Sens.,* **38,** 1260–1276.

Martin, L., M. Schneebeli, and C. Mätzler, 2006: Tropospheric water and temperature retrieval for ASMUWARA. *Meteor. Z.,* **15,** 37–44, doi:10.1127/0941-2948/2006/0093.

Miloshevich, L. M., H. Vömel, D. N. Whiteman, and T. Leblanc, 2009: Accuracy assessment and correction of Vaisala RS92 radiosonde water vapor measurements. *J. Geophys. Res.,* **114,** D11305, doi:10.1029/2008JD011565.

Rodgers, C. D., 2000: *Inverse Methods for Atmospheric Soundings*. World Scientific, 240 pp.

Rosenkranz, P. W., 1998: Water vapor microwave continuum absorption: A comparison of measurements and models. *Radio Sci.,* **33,** 919–928.

Solheim, F., J. R. Godwin, E. R. Westwater, Y. Han, S. J. Keihm, K. Marsh, and R. Ware, 1998: Radiometric profiling of temperature, water vapor and cloud liquid water using various inversion methods. *Radio Sci.,* **33,** 393–404.

Vömel, H., D. David, and K. Smith, 2007: Accuracy of tropospheric and stratospheric water vapor measurements by the cryogenic frost point hygrometer: Instrumental details and observations. *J. Geophys. Res.,* **112,** D08305, doi:10.1029/2006JD007224.

Ware, R., R. Carpenter, J. Güldner, J. Liljegren, T. Nehkorn, F. Solheim, and F. Vandenberghe, 2003: A multichannel radiometric profiler of temperature, humidity, and cloud liquid. *Radio Sci.,* **38,** 8079, doi:10.1029/2002RS002856.